

# ELECTRO-OPTICAL EFFECTS ACCOMPANYING LIGHT PROPAGATION THROUGH AN AEROSOL ATMOSPHERE

V.A. Donchenko

*Siberian Physical-technical Institute, Tomsk, 634050*

*Received August 24, 1988*

*This paper reviews experimental studies of the electro-optical effects accompanying the scattering of optical radiation scattering by aerosols. Different mechanisms for aerosol transformations and anisotropy in an electric field are discussed. The paper also presents some results of investigations into abnormal light scattering and spectral transmission in a medium immersed in a bipolar electric field. We discuss experimental studies of scattered light polarization when aerosol particles are affected by an electric field.*

## Introduction

Electro-optical effects are well studied theoretically and experimentally in gases, dielectrics and condensed media<sup>1,2</sup>. The origin of these phenomena is related to the electromagnetic properties of radiation and matter. It is natural, therefore, to suppose that the optical properties of a medium placed in an electric field would change. Such electro-optical phenomena as the Kerr effect, Pockels effect, and rotation of the polarization plane due to anisotropy induced by a static electric field are already widely used in practice<sup>3,4</sup>. These effects are used to determine the polarizability and conformation of molecules, as well as to study the dynamics of molecular rotation and interactions.

Electro-optics of dispersed media has been developed over the last thirty to forty years, but mainly in applications involving colloid chemistry<sup>5,7</sup>. Certain successes have been achieved in studies of electro-surface phenomena on colloid particles (electronic phenomena, electro-surface forces, double layer). Investigations of these effects have facilitated the development of new diagnostic techniques for dispersed media, including aerosol atmospheres<sup>6,8-10</sup>. It has been also shown that the use of electro-optical effects enables one to determine the shape of particles and the size spectrum (from the value of the rotational diffusion coefficient), and to study the transformation of particle shapes and sizes caused by physical and chemical processes.

An electric field in the earth's atmosphere can significantly change the aerosol properties and aerosol stability, and as a result, the conditions for optical wave propagation in the atmosphere can also change markedly. The basic model of the atmospheric electric field assumes that the atmosphere is a global spherical capacitor, one plate of which is the earth's surface, the other being the upper atmospheric layers. In Ref. 11, one can find a historical description of the investiga-

tions of atmospheric electricity; some information on the present status of this problem can also be found in Refs. 12-14.

The strength of the electric field in the ground atmospheric surface layer can reach  $10^2$  V/m under good weather conditions, and  $10^4$  V/m under poor weather conditions (thunderstorms, snowstorms, duststorms, and other strong atmospheric disturbances). In such a strong field, aerosol particles are practically always electrically charged, and they acquire a charge both during the process of formation and by capturing ions from the air<sup>11,15-19</sup>.

In a polar substance, the dominant influence comes either from an electric double layer related to the surface conductivity, or for an induced dipole moment. Just these properties of particulate matter determine the processes giving rise to the anisotropy and transformations of a dispersed media under the action of an electric field. Since the optical parameters of the atmosphere bear a definite relationship to its electrical parameters, questions of cause and effect, appearing frequently in the literature<sup>12</sup>, can be resolved only taking into account the state of the aerosol and gaseous constituents of the atmosphere<sup>13</sup>.

Normally, the electro-optical phenomena accompanying light scattering by an aerosol atmosphere occur according to the scheme presented in Fig. 1. The growth of electric field power and that of the light field leads to nonlinear electro-optical effects. The theory of both linear and nonlinear effects is still being developed, and not always successfully. The best theoretical successes have been achieved for macromolecules and particles whose sizes are smaller than the wavelength of light<sup>6</sup>.

In the case of larger particles, the theoretical treatment strongly depends on the electro-optical effect considered. The usual analogy with molecules in such a treatment has naturally required significant corrections, and it is often necessary to modify the meaning of some well established concepts<sup>20</sup>.

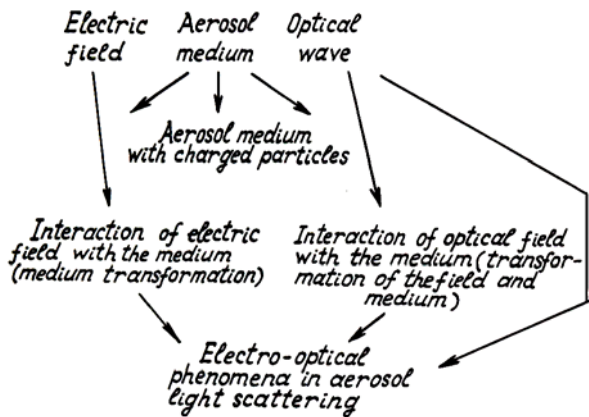


Fig. 1. The origin of electro-optical effects in an aerosol atmosphere.

Electro-optical effects have a number of distinctive features at the moment when the electric field is switched on or off, as do pulsed and alternating electric fields. Alternating fields are usually artificially generated and are used to study the kinetics of electro-optical effects. The use of transients allows for more accurate determination of particle shape and elongation, and of the value and direction of intrinsic and induced dipole moments with respect to the particles axes.

The present review summarizes the experimental results demonstrating the influence of electric characteristics of a volume containing aerosols on its optical characteristics governing the propagation of light. The possible remote determination of the electrical state of the atmosphere based on the use of electro-optical effects is also discussed.

#### ANISOTROPY AND TRANSFORMATIONS OF AEROSOL MEDIA IN A STATIC ELECTRIC FIELD

Light scattering by a homogeneous spherical particle does not depend on the presence of a static electric field inside or outside the particle. But if the particle is of irregular shape, a static electric field ( $E_p$ ) can cause its reorientation by the torques applied. As a consequence, the reorientation of particles modifies the scattering properties of the particle ensemble as a whole.

In the stationary case, electrical reorientation depends on the particle distribution over orientations  $\Omega(\vartheta)^{21-22}$ :

$$n(\vartheta) d\Omega = n_0 \exp(-\Delta U/KT) \sin\vartheta d\vartheta d\varphi \quad (1)$$

where  $\Delta U = 1/2 |\alpha_{\parallel} - \alpha_{\perp}| \sin^2 \vartheta E_p^2$ , the coefficient  $n_0$  is determined from the normalization condition

$$N = n_0 \int_0^{2\pi} d\varphi \int_0^{\pi} \exp(-\Delta U/KT) \sin\vartheta d\vartheta, \quad (2)$$

where  $N$  is the total number of particles in the volume unit,  $K$  is the Boltzmann constant,  $\alpha_{\perp, \parallel}$  is the polarizability of a particle along its principal axis and in the transverse direction. The electric reorientation effect itself is normally characterized by the value  $\alpha_0 = (I_E - I_0)/I_0$  (here  $I_0$  is the intensity of scattered radiation with no electric field,  $I_E$  is the intensity when the electric field is applied).

The oriented effect of an electromagnetic wave involves the fact that during the orientation process, the angle  $\vartheta$  exponentially tends to zero, while the variance of  $\vartheta$  for a stationary orientation is determined by the Boltzmann distribution for the energy of interaction between the induced dipole moment and the field of the wave.

The reorientation of particles in an electric field can occur not only for spherical particles, but also when there is anisotropic internal structure within a particle or on its surface. This also will modify the scattering properties, depending on the particle orientation with respect to the electric vector of the wave. Such anisotropy inside particles can be induced by the external electric field<sup>23</sup>. This can easily be seen in the case of a sea aerosol which, as a rule, is composed of several constituents with different values of the dielectric constant  $\epsilon$ . External electromagnetic or electrostatic fields will produce different ponderomotive forces for particles with different  $\epsilon$  values. As a result the separation of aerosol constituents can take place. This is true, first of all, for an 'external chemical mixture, i.e. for a medium which consists of different chemical substances particulated individually. However there can occur another limiting case of 'internal chemical mixtures' in which the separation would take place within the particles, thus causing their anisotropy.

Physical characteristics of the particles can change, depending on the electric field applied and the chemical composition of the material the particles are made of. This primarily affects the optical constants of the particles. As a consequence, changes in the electric field applied to a medium can cause change its light scattering properties. We have calculated the dielectric constant  $\epsilon_{ss}$  for aerosol media obtained by spraying a water solution of sea salt (basic chemical component NaCl), and for a pure water aerosol. The calculations are also valid for aerosols formed from sea surface sprays<sup>25</sup>. The calculations used the formula<sup>26</sup>  $\epsilon_{ss} = \epsilon_1 + Nf(\epsilon_1, \epsilon_2)$  where  $\epsilon_2$  is the dielectric constant of the dispersed phase,  $N$  is the volume number density of particles,  $f(\epsilon_1, \epsilon_2) = 3(\epsilon_2 - \epsilon_1)\epsilon_1/\epsilon_2 + 2\epsilon_1$ . The variable parameter in these calculations was the volume number density of particles placed in a static electric field ( $E_{const}$ ) and irradiated simultaneously with the electromagnetic field of an optical wave ( $E_{\omega}$ ).

The values of  $\epsilon$  for  $H_2O$  were taken to be 82 for the static field and 1.77 for the optical wave. The expression used for calculations is valid only for low concentrations. The results obtained are presented in Table 1.

Table 1.

$N \times 10^{-8}$	$\epsilon_{ss}(E_{stat})$		$\epsilon_{ss}(E_{\sim})$	
	water fog	sea water fog	water fog	sea water fog
5	1.0005504	1.0005504	1.0005390	1.0005391
10	1.0005649	1.0005648	1.0005421	1.0005422
100	1.0008256	1.0008246	1.0005972	1.0005964
500	1.0019831	1.0019805	1.0008422	1.0008784

As can be seen from this table, the combined action of a static electric field and the alternating electric field of an optical wave on the aerosol medium produces significant changes in the dielectric constant of the medium.

Changes in the polarization state of light result from the anisotropy appearing in the sea water fog due to electrostriction of NaCl crystals. Let us estimate this effect for good weather electric fields in the atmosphere. Particles of NaCl are dielectric crystals with a cubic lattice. This structure is responsible for the isotropy of NaCl optical properties.

However, when placed in an external electric field, the crystal lattice can undergo deformation due to polarization. Under the influence of an external electric field, the center of symmetry of the NaCl crystal lattice disappears and salt particles become anisotropic. If the electric field vector is directed along an edge of the cube, then the size of the crystal lattice increases in this direction, while in the transverse direction it shrinks. Relative changes of size can be written as follows<sup>27,28</sup>:

$$\frac{a_{\parallel}}{a_0} = 1 + R_{1111} E_p^2, \quad \frac{a_{\perp}}{a_0} = 1 + R_{1122} E_p^2 \quad (3)$$

where  $a_0$  is the length of a cube edge with no external electric field applied,  $a_{\parallel}$ ,  $a_{\perp}$  are the edge lengths in directions along and across the external electric field  $E_p$ , respectively;  $R_{1111}$ ,  $R_{1122}$ , are elements of a four-rank tensor ( $R_{1111} > 0$ ,  $R_{1122} < 0$ ). For  $R_{1111} = 0.3 \times 10^{-20} \text{ m}^2/\text{V}^2$ ,  $R_{1122} = -0.15 \times 10^{-20} \text{ m}^2/\text{V}^2$  [28] and for a field strength  $E_p = 400 \text{ V/cm}$ , one obtains  $a_{\parallel}/a_0 = 1 + 8.26 \times 10^{-12}$ ,  $a_{\perp}/a_0 = 1 - 2.07 \times 10^{-12}$ . The change in the dielectric constant of NaCl caused by electrostriction is also insignificant, and for a weak electric field it does not exceed  $10^{-10}$ .

Noticeable deformations of crystals should be anticipated in strong static and electromagnetic fields. In strong electromagnetic fields, surface vibrations of water droplets can occur due to ponderomotive forces, and aspherical particles can become oriented as they are accelerated through the air. In either case, lidar returns from randomly or regularly oriented ensembles of particles are altered<sup>29</sup>.

More significant perturbations of particle shapes occur when an electric field is applied to a medium with enhanced conductivity. Before there are ions in

the medium, charged particles repel each other and, as a consequence, no coagulation occurs. But as the number of ions in the medium increases, coagulation can take place, since ionic screening of a particle locally reduces the external electric field around it, allowing collisions between particles and cluster formation.

Scattering properties of the medium (e.g. scattering cross section) can also change due to interaction between an external electric field and charged aerosol particles<sup>31,32</sup>. These changes are related to the behavior of free mobile excess charges on the particle surface. However, real atmospheric solid aerosols are mostly irregularly shaped, hampering free surface movement of charges; at the same time, there is little reliable information on charge movement inside a particle.

For this reason the effects of resonant light scattering by naturally occurring charged particles are very difficult to interpret.

Thus, in this section we have tried to intuitively select from the many possible mechanisms those likely to produce electrooptical effects, taking the physical conditions into account. Some instances in which an electric field appears as a result of processes occurring in the light beam itself have been analyzed in Ref. 33.

### SPECIFIC FEATURES OF THE ANGULAR DISTRIBUTION OF SCATTERED RADIATION IN A BIPOLAR CHARGED MEDIUM

Light scattering in the forward direction. Investigations of forward scattering in different kind of wood smoke (having different conductivity) are presented in Ref 30. Ionization of the medium was produced by the corona discharge from the corners of a capacitor plate. The strength of the static electric field applied to the medium was chosen to be close to that in the free atmosphere, and to typical values under thunderstorm conditions.

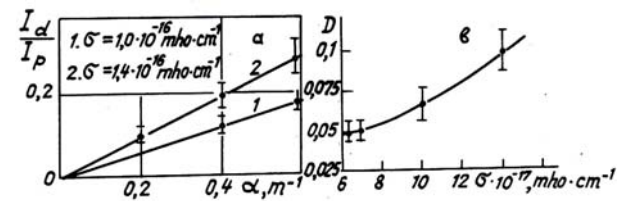


Fig. 2. Experimental data for the ratio  $I_{sc}/I_p$  measured at different values of the extinction coefficient: dependence of  $I_{sc}/I_p$  on the medium's conductivity.

The measurements were carried out in a special chamber for artificial media. Static electric fields were produced by a plane capacitor. Some results of these measurements are presented in Fig. 2a. This figure presents the ratio of scattered to unscattered radiation intensity ( $J_{sc}/J_p$ ) as a function of the medium's extinction coefficient at  $\lambda = 0.63 \mu\text{m}$ . Line 1 presents the data obtained with no additional electric field and ionization at natural conductivity  $\sigma = 10^{-16} \text{ mho/cm}$ . Line 2 presents the data obtained in the case of en-

hanced ionization in the chamber with  $\sigma = 1.4 \times 10^{-16}$  mho/cm. The values

$$D = 1 / 2 \int_0^{\Psi} \int_0^{\Theta} x(\rho, \Psi + \Theta) d\Psi d\Theta$$

determining the fraction of the forward scattered radiation were 0.07 and 0.1, respectively, for these two cases. Here  $\Theta$  and  $\Psi$  are the sounding beam divergence and the receiver's field of view, respectively,  $x(\rho, \Psi + \Theta)$  is the aerosol scattering phase function, and  $\rho$  is the Mie parameter. Thus one can see from these results that the  $D$  value can be accounted for by changes in the aerosol structure depending on the number of ions, and thus on the medium's conductivity. The value of the Mie parameter determined by comparing the experimental and theoretical values of  $D$  in the above cases ranged from 1 to 2 and 4 to 5, respectively. This corresponds to a growth in particle size from 0.2 to 0.4  $\mu\text{m}$ . The growth of particles is due to coagulation. Measurements of the forward scattered radiation at different conductivities of the medium enable one to study the dynamics of the coagulation process. The experimentally measured dependence of  $D$  on  $\sigma$  is presented in Fig. 2b. It is seen from this figure that at low  $\sigma$  values this fraction of the forward scattered radiation remains constant; it then varies slightly for  $\sigma$  between  $7 \times 10^{-17}$  mho/cm and  $9 \times 10^{-17}$  mho/cm. An abrupt increase in the  $D$  value takes place at  $\sigma > 10^{-16}$  mho/cm, signaling the onset of the coagulation process.

Ref. 34 presents the results of measurements made in wood smoke which show the optical effects of particle asphericity occurring during the coagulation process. The authors of this paper measured the electro-optical response of the medium at  $45^\circ$  scattering angle. The electro-optical parameter  $\alpha_0$  can rise or fall in magnitude with time, depending on the asphericity of the coagulated clusters, but in 30 to 40 minutes from the beginning of combustion it always reaches a saturation level.

The strength of the electric field in an aerosol atmosphere as well as its sign are also influenced by the volume charge of particles  $\rho_e \text{ cm}^3$ . Changes of the volume charge due to ionization result in changes of the surface potential of particles that can lead to transformations of the aerosol medium as well. Light scattering under such conditions has been studied in Ref. 16, where the equilibrium ionic charge on water droplets growing on insoluble nonionogen (AgI) and on soluble ionogen (NaCl) condensation nuclei in bipolar ionized air was studied.

Figure 3a presents the intensity ratio  $J(4^\circ)/J(45^\circ)$  (curves 1 and 1') for scattered radiation as a function of relative humidity between 30 to 100%. Note that this intensity ratio is sensitive to changes in particle size.

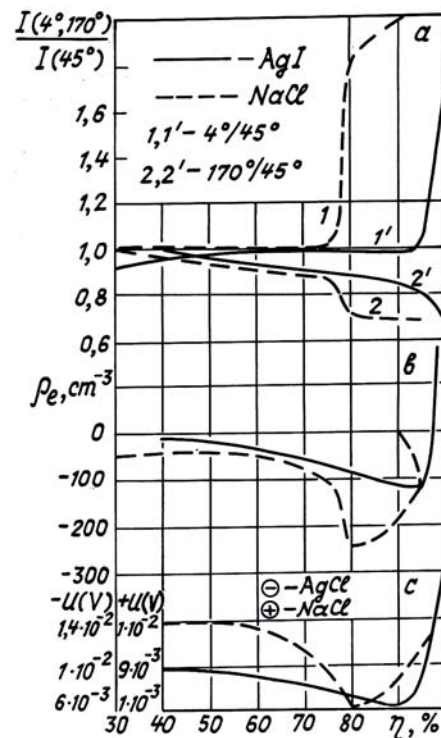


Fig. 3. Dependence of intensity ratios  $I(4^\circ)/I(45^\circ)$ ,  $I(170^\circ)/I(45^\circ)$ , volume charge and surface potential of particles on air humidity.

Figure 3b and 3c show the behavior of the volume charge  $\rho$  during the transformation of particles and the surface potential of droplets calculated for these conditions.

As is seen from these figures, an abrupt change in scattering cross-section and volume charge is a common feature of both these characteristics under certain conditions. The intensity of the scattered radiation for relative humidity between 30 and 80 percent is determined by the volume charge of water-soluble particles at the stage of water vapor absorption on the surface of the solid nucleus, when the latter are NaCl and AgI (curves 1 and 1'). Furthermore, there exist two more stages in which particle sizes and scattering cross-sections change for NaCl particles, namely the condensation growth of a particle and condensation growth of a droplet of dilute solution.

Light scattering in the backward direction. It is necessary in lidar sensing of the atmosphere to take into account gradients of atmospheric humidity and variations in the electric field, as both of these factors contribute to coagulation processes. In Ref. 35 an experimental study was made of the dependence of backscattering coefficients  $\beta_\pi$  of small particles of wood smoke on relative humidity in an external static electric field. The results of these investigations are presented in

Fig. 4 for a medium with extinction coefficient  $\alpha_{ext}$  ( $\lambda = 1.06 \mu\text{m}$ ) is equal to  $0.13 \text{ m}^{-1}$ . It is seen from this figure that with no external electric field, the backscattering coefficient slowly increases, beginning at a relative humidity of 60%. When an external electric field is applied to the medium, one can observe a two- to fourfold increase in the backscattering coefficient for electric field strengths from 250 to 450 V/cm. It is interesting that the rate of  $\beta_\pi$  growth is larger at a relative humidity of 30 to 40 percent. In the absence of an external electric field, backscattering coefficient growth with increasing relative humidity from 30 to 90 percent is due to coagulation of particles caused by capillary forces. The wood smoke particles themselves are electrically charged as they are produced, so increasing relative humidity can lead to various electric effects on the particles surfaces (oriented adsorption of water molecules on the surface, charging and recharging of particles, polarization of charges on particles and so on). Consequently, induced charges can appear on the moistened particles. This explains the dipole charging of particles and enhancement of the agglomeration probability. The effect is most pronounced for small particles between 0.01 and 0.1  $\mu\text{m}$  in diameter<sup>36</sup>. An external electric field causes additional charging of aerosol particles by surface capture of ions from the air. As a result, there is an additional drift of charged particles in the external electric field. These processes enhance coagulation and growth of particles. The backscattered signal then also increases in magnitude. A simultaneous increase in humidity and electric field strength leads to a sharp increase in backscattered radiation intensity.

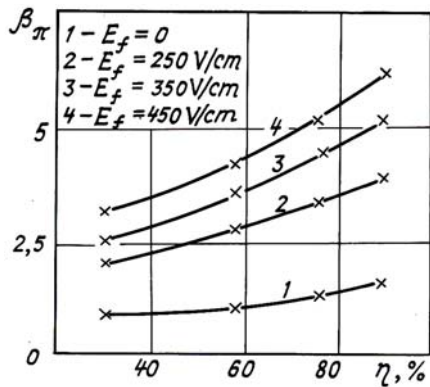


Fig. 4. Backscattering coefficient' as a function of air humidity at different electric field strengths.

Measurements of the intensity ratio  $J(170^\circ)/J(45^\circ)$ , which is more sensitive to changes in the refractive index as a function humidity when the volume charge varies, are presented in Fig. 3a (curves 2 and 2') [16]. It should be noted that the behavior of this intensity ratio is probably a mirror image of the  $J(4^\circ)/J(45^\circ)$  ratio behavior. This peculiarity, first detected experimentally by Savchenko [16], can probably be used for solving inverse problems.

In Ref. 32 Simonov et al report on the reflection of superhigh frequency radiation from a cloud of charged

ammonium chloride particles. Observed scattering cross-sections are smaller than  $\sigma_{c1} = \sigma_{geom} f(c_{ss})$  (where  $\sigma_{geom}$  is the geometrical cross-section of the cloud). The authors of this paper explain the difference by the anomalous resonant scattering of radiation by aerosol particles which they consider to be most probable in this case. The anomalous scattering of electromagnetic radiation with matter requires further study.

### POLARIZATION OF OPTICAL RADIATION SCATTERED FROM PARTICLES IN AN ELECTRIC FIELD ON PARTICLES

Polarized and cross-polarized components of scattered radiation are sensitive to modifications of a medium due to an external electric field. Figure 5a presents measurements of the degree of polarization for radiation reflected from coastal hazes at different relative humidity values  $\eta$ <sup>37</sup>. The degree of polarization is close to zero, and can even be negative. Particle asphericity fails as an explanation of such strong depolarization, because the microphysical measurements that were made showed that particles formed by crystallization from solution droplets had irregular but mostly isometric shapes. Negative degree of polarization for backscattered radiation were also observed in Refs. 38, 39, where the polarization properties of aerosols above water and in the stratosphere were studied. The authors of these papers explain this phenomenon by the occurrence of anisotropic layers formed by wind shear and other smoothing processes in the atmosphere.

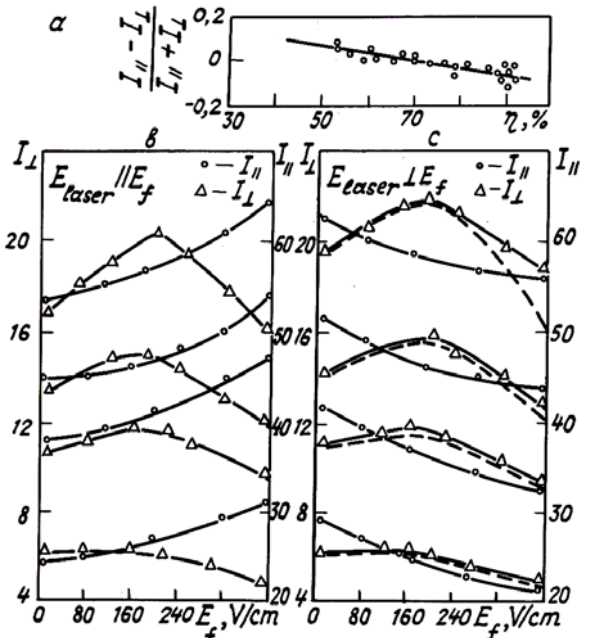


Fig. 5. Degree of polarization of backscattered radiation as a function of air humidity and dependencies of polarization components on electric field strength for sea salt: b) for  $E_0 \parallel E_p$ , c)  $E_0 \perp E_p$ , curves 1-4 are for  $I_{\perp}$  and 1'-4' are for  $I_{\parallel}$ , dashed curves show calculations of  $I_{\perp}$ .

An analysis of the meteorological situation in which the measurements<sup>37</sup> were made showed that the electric field could be one of the factors causing particle orientation. By that time, information was available from the literature on electro-optical effects in NaCl particles<sup>40</sup>. For that reason the authors of Ref. 41 assessed the possible impact of this factor, as well as that of the natural electric field of the Earth, on the polarization of scattered radiation.

The theoretical model describing the dependence of backscattered optical polarization on electric field strength assumes that anisotropic particles of the aerosol in question are isometric. There are also certain limitations imposed in this model on the polarizability tensor which are equivalent to the assumption that the particles are uniaxial both at low and optical frequencies.

The principal elements of the polarizability tensor in a static electric field  $\alpha_{ij}$  obey the relationships  $\alpha_{11} = \alpha_{22} = \alpha_{\perp}$ ;  $\alpha_{33} = \alpha_{\parallel}$ . Analogous conditions are imposed on the  $\beta_{ij}$  tensor (i.e.  $\beta_{11} = \beta_{22} = \beta_{\perp}$ ,  $\beta_{33} = \beta_{\parallel}$ ), which describes the anisotropy of the polarizability at optical frequencies. It is also assumed that the directions of  $\alpha_{\parallel}$  and  $\beta_{\parallel}$  coincide, while the relationships between other components of the  $\alpha_{ij}$  and  $\beta_{ij}$  tensors can be arbitrary. The model excludes orientation of particles by the incident radiation. Calculations using this model give the following expressions describing the intensity of parallel and cross-polarized components of radiation scattered per unit volume as functions of the electric field strength  $E_p$ , when the electric vector of incident radiation is parallel to  $E_p$ :

$$J_{\parallel}(\xi) = \frac{N k^4 \epsilon_0 \langle E_0^2 \rangle c}{16\pi r^2} \left\{ |\beta_{\parallel} - \beta_{\perp}|^2 \times [F_2(\xi) - F_1(\xi)] + |\beta_{\parallel}|^2 F_1(\xi) + |\beta_{\perp}|^2 [1 - F_1(\xi)] \right\}$$

$$J_{\perp}(\xi) = \frac{N k^4 \epsilon_0 \langle E_0^2 \rangle c}{16\pi r^2} |\beta_{\parallel} - \beta_{\perp}|^2 [F_1(\xi) - F_2(\xi)] \quad (4)$$

where  $\xi = (\epsilon_0 |\alpha_{\perp} - \alpha_{\parallel}| / KT)^{1/2} E_p$ , and  $r$  is the distance from the receiver to the scattering volume. The dimensionless functions  $F_1(\xi)$  and  $F_2(\xi)$  are given by

$$F_1(\xi) = \int_0^{\xi} \exp(y^2) y^2 dy \left[ \xi^2 \int_0^{\xi} \exp(y^2) dy \right]^{-1}$$

$$F_2(\xi) = \int_0^{\xi} \exp(y^2) y^4 dy \left[ \xi^4 \int_0^{\xi} \exp(y^2) dy \right]^{-1} \quad (5)$$

These are increasing functions and they tend to unity as  $\xi \Rightarrow \infty$  with their difference being maximum

at  $\xi = 1.45$ . The above model of electrooptical effects caused by external electric fields in spherical anisotropic particles admits of the following interpretation of the maximum in the intensity of the cross-polarized backscattered component as a function of external field strength<sup>21</sup>. At low values of the external field strength, only partial orientation of particles occurs, and at certain values there exist a predominant orientation angle. When this takes place, the value  $J_{\perp}$  reaches its maximum. Further increases in the field strength  $E_p$  force more and more particles to orient along  $E_p$ , and as a result  $J_{\perp}$  decreases.

Modeling experiments have been carried out in fogs obtained by spraying a 3.5 per cent solution of sea salt. The percentage of the solution was based on the salinity of the world's oceans. Relative humidity of air was kept constant at  $\eta = 40\%$ . The intensity of polarized components of radiation ( $\lambda = 1.06 \mu\text{m}$ ) scattered at  $187^\circ$  was measured relative to the incident intensity.

Experimental and calculated data are presented in figures 5b and 5c. The intensity  $J_{\perp}$  always has a maximum as a function of field strength, consistent with the above interpretation. The intensity of the polarized component  $J_{\parallel}$  depends upon whether  $E_0$  is parallel to  $E_p$  or perpendicular to it. The difference between these cases is fully accounted for within the framework of the above model. The relation between the absolute values of the principal values of the polarizability tensor  $\beta_{\parallel}$  and  $\beta_{\perp}$  and the absolute value of their difference determines what kind of behavior takes place. Calculated dependencies  $J_{\parallel}(E_p)$  are shown in Fig. 5c by dashed curves. That figure shows that there are significant differences between experiment and theory in some cases at large  $E_p$  values, indicating that there may be other new mechanisms resulting in optical anisotropy besides changes of the dipole properties of particles.

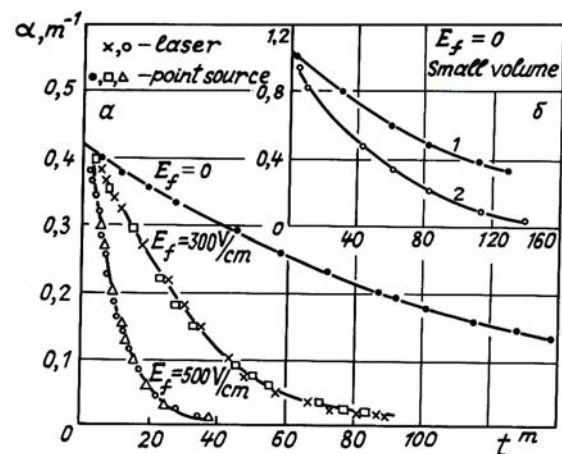


Fig. 6. The dynamics of ionized smokes dissipation in electric field.

#### SPECTRAL TRANSMISSION OF A BIPOLAR IONIZED MEDIUM

Let us consider the dynamics of changes in the extinction coefficient of wood smoke at  $\lambda = 0.63 \mu\text{m}$

for a static external electric field, for the field produced by a corona discharge, and for a laser spark. Experiments have been carried out in large and small (50×50×50) cm<sup>3</sup> chambers in cooperation with Yu.I. Kulakov and E.V. Lugin. Ionization of the medium in the small chamber was initiated by a CO<sub>2</sub> laser spark at one point in the chamber.

Temporal behavior of the extinction coefficient for optical radiation is shown in Fig. 6a for three values of electric field strength  $E_p = 0, 300, \text{ and } 500 \text{ V/cm}$ . With no external field or discharge, the extinction coefficient  $\alpha, \text{ m}^{-1}$  changes very slowly, and the process of smoke dissipation lasts takes about six hours. Switching on the ionization source and application of the external electric field causes more rapid changes in  $\alpha$  due to faster dissipation of smoke. Thus at a field strength  $E_p = 300 \text{ V/cm}$ , the dissipation of smoke took about 100 minutes, while at  $E_p = 500 \text{ V/cm}$ , it took only 40 minutes. Conductivity of the medium inside the chamber ranged from  $7 \cdot 10^{-17} \text{ mho/cm}$  at  $E_p = 0$  to  $1.7 \cdot 10^{-16} \text{ mho/cm}$  at  $E_p = 500 \text{ V/cm}$ . The temporal behavior of  $\alpha$  in the small chamber at  $E_p = 0$  but ionized with a laser spark, is illustrated by Fig. 6b. Curve 1 in this figure presents the  $\alpha$  behavior with no ionization source while curve 2 presents the opposite case, where there is an ionization source inside the chamber. Again the presence of additional ions in the medium gives rise to a marked decrease in the smoke dissipation time. The behavior of the particle concentration in the case of electro-coagulation, taking account of the probability of charged-particle collisions and electrostatic dissipation, can be described by<sup>15</sup>

$$\frac{dN}{dt} = K_1 [(N_+^2 + N_-^2) p_1 + 2N_+ N_- p_2] = \frac{4\pi q_1 q_2 D_d}{KT} \quad (6)$$

Here  $K_1 = 8\pi R D_d$  is the coefficient of Brownian coagulation;  $p_1 = \gamma(e^{\gamma} - 1)^{-1}$  and  $p_2 = \gamma^2(e^{\gamma} - 1)^{-1}$  are the probabilities of collisions between particles of like and opposite charges, respectively;  $\gamma = q_1 q_2 / (2RKT)$ , where  $q_1$  and  $q_2$  are the charges on interacting particles;  $N_+$  and  $N_-$  are the numbers of positively and negatively charged particles, respectively. If one assumes that  $N_+ = N_- = N/2$ , then it is possible to write the ratio of rates of concentration changes for charged and uncharged aerosols as

$$m = \frac{\gamma \exp(\gamma)}{\exp(\gamma) - 1} - \frac{\gamma}{2} > 1 \quad (7)$$

Equation (7) shows that the rate of coagulation of charged particles is higher than that of uncharged particles. Thus, additional ionization of a medium by corona or spark discharge increases the efficiency of the coagulation process.

Consider now the behavior of the extinction coefficient  $\alpha_{\text{ext}}(\lambda)$  during electrocoagulation, since the particles' shape, size, size distribution and number density will all be changing. Neglecting changes in particle shape, one can write

$$\frac{dN}{dt} = -K_1 N^2 - \alpha_{\text{ext}}(\lambda) N. \quad (8)$$

The second term in this equation describes the processes accompanying natural Brownian coagulation. Consider in our case the influence of an electric field on polarization coagulation, i.e. when  $\alpha = \alpha(E_p)$ . If one neglects the effect of frequency dependence of the field on coagulation, i.e., one assumes that the electric field is static, then the solution of equation (8) will take the form

$$\frac{N - \frac{\alpha_{\text{ext}}(\lambda) + K_1 N_0}{\alpha_{\text{ext}}(\lambda) + K_1 N_0}}{N_0 - \frac{\alpha_{\text{ext}}(\lambda) + K_1 N_0}{\alpha_{\text{ext}}(\lambda) + K_1 N_0}} = \exp[-\alpha_{\text{ext}}(\lambda) t], \quad (9)$$

where  $N_0$  is the concentration of particles at  $t = 0$ . Assuming that  $\alpha(E) = t_0^{-1}$ , one obtains from (9)

$$N = \frac{N_0 \exp(-t/t_0)}{1 + K_1 t_0 N_0 [1 - \exp(-t/t_0)]} \quad (10)$$

Since Brownian coagulation takes place efficiently at very high densities of uncharged particles, it can be neglected. Then

$$N = N_0 \exp(-t/t_0) \quad (11)$$

where  $t_0 = 1/\alpha(E_p)$  is the effective coagulation time. Time  $t_0$  is determined by the natural electric field of the atmosphere, whose strength  $E_0$  always exceeds zero.

Therefore, one can obtain the following expression for the extinction coefficient:

$$\alpha_{\text{ext}}(\lambda) = N_0 \exp(-t/t_0) \int_0^{\infty} \sigma(R, \lambda) f(R) dR \quad (12)$$

Assuming that  $t_0 = t_{\text{eff}} \exp(-\nu E_p/E_0)$  (here  $t_{\text{eff}}$  is the effective aerosol dissipation time, and  $\nu$  is a dimensionless coefficient depending on the medium properties), and bearing in the mind that coagulation only weakly affects the shape of the  $f(R)$  function in smoke<sup>30</sup>, one obtains

$$\alpha_{\text{ext}}(\lambda) = \alpha_{0\text{ext}}(\lambda) \exp\left[-\frac{t}{t_{\text{eff}} \exp(-\nu E_p/E_0)}\right] \quad (13)$$

It follows from the experimental data presented in Fig. 6 that  $t_{\text{eff}}$  is the time during which  $\alpha_{0\text{ext}}(\lambda)$  decreases by a factor of  $e$  if no electric field is applied, and  $\nu = 6 \cdot 10^{-3}$ .

Figure 7 presents the time behavior of the extinction coefficient  $\alpha_{\text{ext}}(\lambda)$  with an external electric field  $E_p = 450 \text{ V/cm}$  for different initial densities of smoke. Curves in this figure represent data calculated using expression (13), while dots represent the experimentally measured values. Good agreement between the numerical and experimental data shows the validity of the assumptions adopted in deriving the expression for  $\alpha_{\text{ext}}(\lambda)$ .

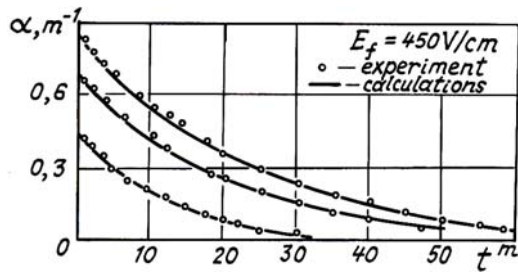


Fig. 7. Dissipation dynamics of ionized smoke in an electric field for different initial densities of smoke.

An increase in the velocity of charged aerosol particles in an electric field (the electro-filtration effect) can also result in electro-optical phenomena. Electro-filtration can produce a situation in which the transparency of two adjacent channels can differ. Studies of this effect have been carried out in a chamber 1 m long for fogs obtained by water evaporation. One of the chamber walls was made of transparent plastic, which could be statically charged. The electric field distribution inside the chamber is shown in Fig. 8a.

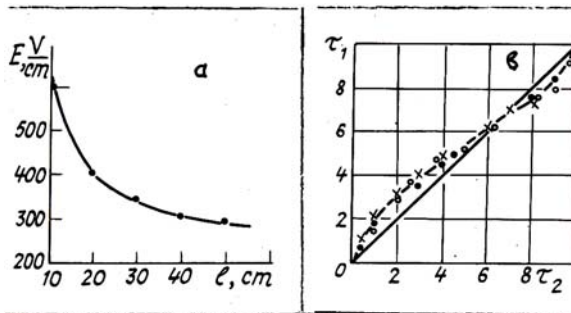


Fig. 8. a) The effect of electro-filtration on optical depth. b) The static electric field distribution inside the chamber.

The abscissa in this figure is the distance from the chamber wall while the ordinate is the strength of the electric field. The distance from the wall to the nearest light source was 15 cm, and that between two sources was 20 cm. Measured values of the optical depth are presented in Fig. 8b. Subscript 1 denotes the data obtained for the channel nearest the wall while subscript 2 denotes the data for the second channel. As can be seen from the figure, at the initial time the number density of particles in the second channel is lower than in the first, due to intensive drift of particles toward the latter. At  $\tau \approx 5$  to 7, the signals through the two channels become equal, and the first channel then becomes the more transparent. In these measurements, the maximum difference between the two channels was  $\Delta\tau = 1$ . It is worth nothing that in the real atmosphere this effect might be masked by turbulent mixing of particles; nevertheless, it can still cause additional fluctuation of atmospheric transparency.

## CONCLUSION

Studies of electro-optical phenomena accompanying light propagation through the atmosphere are only in the initial stages of finding basic regularities. Other interesting mechanisms of electric field influence on the interaction between optical waves and the media they propagate through exist as well. Thus, for example, in Ref. 12 the mechanism of influence of ions on the extinction of IR and submillimeter waves in a bipolar medium is considered. The mechanism is related to the formation of metastable particles with sizes from  $10^{-7}$  to  $10^{-4}$  cm resulting from a radiolysis reaction. Many years' observations of atmospheric electricity<sup>11</sup> have made it possible to establish the relationship between electric field strength  $E_p$  and meteorological visual range  $S_m$  in the form  $E_p S_m = \text{const}$ . This relationship is the result of the influence of humidity and atmospheric turbidity on the atmospheric electric field. The nature of this influence is still unclear, and this relationship is valid only for certain special states of the atmosphere.

Many problems of atmospheric physics require one to find new ways of using the electric properties of the atmosphere in studies of atmospheric pollution on local and global scales. In some of these problems, one wishes to measure the electric properties of the atmosphere using lidar techniques. Remote measurements of the electric field strength can be made, e.g., using CARs techniques<sup>42</sup>. But this method is inefficient for media with strong absorption and scattering of light. The data reviewed in this paper can provide a basis for developing remote methods of measuring the electric field strength in aerosols. Such techniques are needed for investigations into electric properties of the middle atmosphere which play an important role in weather forecasting, as well as for remote optical sensing of the underlying surface<sup>43</sup>.

Utilization of the dependence of polarization parameters of backscattered radiation (of Stokes parameters, generally speaking) on the strength of an external electric field capable of orienting the aerosol particles supplements studies of aerosols using pulsed electric fields. These methods enable one to assess the polarizability of particles in a static electric field and to find the form of the optical polarizability tensor. Both of these parameters are sensitive to aerosol transformations caused by atmospheric conditions.

Our analysis demonstrate the necessity of taking account of the interaction between static electric fields and aerosol media in problems of optical wave propagation through the atmosphere, as well as in problems of lidar data interpretation. This, in turn, requires additional theoretical and experimental data on scattering matrices for nonspherical and anisotropic particles. In this regard, questions of light scattering by a system of randomly oriented particles of different shapes should be solved taking into account new techniques, specifically those related to calculating the scattering characteristics of such ensembles of particles. A combined solution of the foregoing problems

could make it possible to measure the electro-optical parameters of the atmosphere, which in turn characterize its electrical properties.

### REFERENCES

1. S. Kellih *Linear Molecular Optics* (Nauka, Moscow, 1981)
2. M.F. Vuks *Electrical and Optical Properties of Molecules and Condensed Media* (Izdat. LSU, Leningrad, 1984)
3. A.N. Vereshchagin *Polarizability of Molecules*. (Nauka, Moscow, 1980)
4. V.V. Prezhdo, M.V. Khashchina, and V.A. Zamkov *Electro - Optical Research in Physics and Chemistry*. (Izdat. KhSU, Kharkov, 1982)
5. D.A. Fridrihsberg *The Course in Colloid Chemistry* (Khimia, Leningrad, 1984)
6. S. Stoilov, V.N. Shilov, S.S. Dukhin, S. Sokerov and I.V. Petrauchin *Electro-Optics of Colloids* (Kiev, Naukova Dumka, 1977)
7. S.S. Dukhin, V.R. Estrella-Liupis and E.K. Zholnovskii *Surface Electric Phenomena and Electrofiltration*. (Kiev, Naukova Dumka, 1985)
8. V.N. Kapustin, Yu.S. Lyubovtseva and G.V. Rosenberg *Izvestiya Akad. Nauk SSSR ser. Fiz. Atmos, i Okeana*, **11**, 1015 (1975)
9. V.N. Kapustin, V.A. Zagainov and N.T. Shirina *Izvestiya Akad. Nauk SSSR, ser. Fiz. Atmos, i Okeana*, **16**, 261 (1980)
10. V.N. Kapustin, Yu.S. Lyubovtseva, S.P. Stoilov and I.V. Petrauchin *Izvestiya Akad. Nauk SSSR, ser. Fiz. Atmos, i Okeana*, **19**, 696 (1983)
11. Yu.I. Frenkel and K.S. Shifrin *The Theory of Atmospheric Electricity Phenomena*. (GITL, Leningrad, 1949)
12. I. M. Imyanitov and K.S. Shifrin *Usp. Fiz. Nauk*, **76**, 593 (1962)
13. V.V. Smirnov *Trudy. Hidro. Met. Inst.*, No. 30(104), 64 (1983)
14. Yu.A. Bragin in: *Computer Application in the Atmospheric and Ionospheric Physical Processes Investigation* (Izdat. GGI, Novosibirsk, 1987)
15. H. Green and V. Lane *Aerosols, Dust, Smokes, Fogs*. (Khimia, Leningrad, 1982)
16. A.V. Savchenko *Trudy Hidro. Met. Inst.*, No. 24(89), 38 (1980)
17. N.V. Krasnogorskaja *Electricity in the Lower Atmosphere and Methods for its Measurements* (Gidrometizdat, Leningrad, 1984)
18. V.M. Muchnik *Physics of Thunderstorm* (Gydrometizdat, Leningrad 1984)
19. V.M. Muchnik and B.E. Fishman *Electrization of coarse aerosol fraction in the atmosphere* (Gydrometizdat, Leningrad 1982)
20. S.S. Dukhin and V.N. Shilov *Dielectric phenomena and double layer in dispersed Media and polyelectrolits* (Naukova Dumka, Kiev, 1972)
21. V.E. Zuev and M.V. Kabanov *Optics of Atmospheric Aerosol* (Gydrometizdat, Leningrad, 1982)
22. B.V. Kaul *Izv. Vyssh. Ucheb. Zaved. Flzika*, No.11, 17, (1983)
23. A.S. Vyalkin, V.A. Donchenko, M.V. Kabanov and N.A. Stakhin in: *Proc. IX All-Union Symp.on Laser Propagation in the Atmosphere*. (Izdat. TFSO Akad. Nauk SSSR, Tomsk, 1987)
24. A.S. Vyalkin, V.A. Donchenko, M.V. Kabanov and N.A. Stakhin in: *Proc. VIII All-Union Symp. on Laser Propagation In the Atmosphere*, part 1 (Izdat. TFSO Akad. Nauk SSSR, Tomsk, 1986)
25. Yu.V. Zhulanov and I.V. Petryanov *Dokl. Akad. Nauk SSSR*, **253**, 845 (1980)
26. L.D. Landau and E.M. Lifshits *Electrodynamics of continious media* (Nauka, Moscow, 1982)
27. Yu.I. Sirotnin and M.P. Shaskolskaya *General Crystallography* (Nauka, Moscow, 1979)
28. I.S. Zheludev *Physics of crystal dielectrics* (Nauka, Moscow, 1968)
29. Yu.D. Kopytln, G.A. Mal'tseva and S.A. Shishigin in *Sensing of Physico-Chemical Parameters of the Atmosphere Using High Power Lasers* (Izdat. IOA, Tomsk, 1979)
30. V.N. Genin, V.A. Donchenko, M.V. Kabanov et. al. *Izv. Vyssh. Uchebn. Zaved. Fiz.* **29**, No. 2, 82 (1986)
31. A.A. Lushnikov, V.V. Maksimenko, A.Ya. Simonov and A.G. Sutugin *Izv. Vyssh. Uchebn. Zaved. Radiofiz.* **27**, No. 726 (1984)
32. A.Ya. Simonov *Izv. Vyssh. Uchebn. Zaved. Radiofiz.* **31**, No. 1, 62 (1988)
33. V.P. Ageev, S.G. Burdin, I.N. Goncharov, V.F. Konov, I.M. Minaev and N.I. Chapliev *Interaction of high-power pulsed laser radiation with solid particles in gases*, in: *Radiotekhnika*, Vol. **31**, (VINITI, Moscow, 1983)
34. V.N. Kapustin and A.A. Korneev *Izvestiya Akad. Nauk SSSR, ser. Fiz. Atmos, i Okeana*, **24**, 280, (1983)
35. V.A. Donchenko, M.V. Kabanov, Yu.F. Kulakov and V.P. Petrov in *Proc. IX All-Union Symposium on laser propagation in the atmosphere*, Tomsk (Izdat. TFSO Akad. Nauk SSSR, Tomsk, 1987)
36. L.S. Ivlev *Chemical Composition and Structure of Atmospheric Aerosols*. (Izdat LSU, Leningrad, 1982)
37. V.A. Donchenko, Yu.F. Kulakov and V.P. Petrov in: *Electro-dynamics and wave propagation, part 2* (Izdat. TSU, Tomsk, 1982)
38. W.R. Menial and A.I. Carswell *Appl. Opt.* **14**, 2158 (1975)
39. V.E. Derr, N.Z. Abshire, R.E. Cupp and I.T. Menice *J. Appl. Met.* **15**, 1200, (1976)
40. V.N. Kapustin, Yu.S. Lyubovtseva, in: *Proc. All-Union Meeting on Atmosheric Optics* (Izdat IOA, Tomsk, 1976)
41. V.A. Donchenko, M.V. Kabanov, B.V. Kaul and Yu.F. Kulakov *Izvestiya Akad. Nauk SSSR, ser. Fiz. Atmos, i Okeana*, **16**, 1173, (1985)
42. M.A. Buldakov, N.F. Vasiliev, S.V. Lazarev and I.I. Matrosov *Kvant. Elektron.*, **11**, 405 (1984)
43. V.A. Donchenko, V.E. Zuev, M.V. Kabanov et al. *Electrodynamics and wave propagation*. (Izdat. TSU, Tomsk, 1987)